

Cellular solid behaviour of liquid crystal colloids

2. Mechanical properties

V.J. Anderson and E.M. Terentjev

Cavendish Laboratory, University of Cambridge, Madingley Road, Cambridge CB3 0HE, U.K.

October 28, 2018

Abstract. This paper presents the results of a rheological study of thermotropic nematic colloids aggregated into cellular structures. Small sterically stabilised PMMA particles dispersed in a liquid crystal matrix densely pack on cell interfaces, but reversibly mix with the matrix when the system is heated above T_{ni} . We obtain a remarkably high elastic modulus, $G' \geq 10^5$ Pa, which is a nearly linear function of particle concentration. A characteristic yield stress is required to disrupt the continuity of cellular structure and liquify the response. The colloid aggregation in a “poor nematic” MBBA has the same cellular morphology as in the “good nematic” 5CB, but the elastic strength is at least an order of magnitude lower. These findings are supported by theoretical arguments based on the high surface tension interfaces of a foam-like cellular system, taking into account the local melting of nematic liquid and the depletion locking of packed particles on interfaces.

PACS. 61.30.-v Liquid crystals. – 82.70.-y Disperse systems. – 81.40.Jj Elasticity and anelasticity, stress-strain relations.

1 Introduction

In the preceding paper [1] we have described the structure and aggregation mechanisms of thermotropic nematic colloid with a new cellular morphology. We argued that, in some circumstances, the continuous phase separation takes place, driven by the mean field energy of orientational nematic order in the matrix. This mechanism, and the resulting cellular structure with colloid particles densely packed on thin interfaces, is different from a number of previous observations [2, 3, 4, 5]. In those cases particles always aggregated into dense 3-dimensional flocs, often supported by line or point disclinations.

We showed that the behaviour of a liquid crystal colloid is determined by the dimensionless parameter WR/K , where W is the nematic anchoring energy on the particle surface, K the Frank elastic constant¹ and R the particle radius. A spherical colloid particle in a nematic liquid crystal creates a topological defect in the director field, if $WR/K \gg 1$. When this parameter is small (which is our case, with PMMA particles of $R \sim 150$ nm), the particle introduces only a small perturbation into the nematic matrix. In this case the long range interaction forces between particles are sufficiently weak so that the aggregation times are long compared with the alternative mechanism of continuous phase separation. Direct observation in the bulk of our samples with the confocal microscopy

¹ For typical thermotropic nematics and homeotropic director anchoring used in our work, these material constants take the values $W \sim 10^{-6}$ J/m² and $K \sim 10^{-11}$ J/m, e.g. [6].

technique have confirmed the open-cell morphology and the estimate for the cell size of the structure, $\lambda \sim (nR)/\Phi$, where nR is the wall thickness and Φ the average particle concentration, (experimentally we find $n \sim 20 - 30$, [1]). Recently Tanaka *et al.* [7] studied phase separation in mixture of a 5CB nematic and a surfactant, which forms very small micelles. They reported some provocative results, also quite different from ours. We could speculate that, in their case, the colloid parameter WR/K is so small that the mechanism of phase separation described in [1] is not valid, indeed, nano-micelles might be too small to apply any mean-field description of a nematic order.

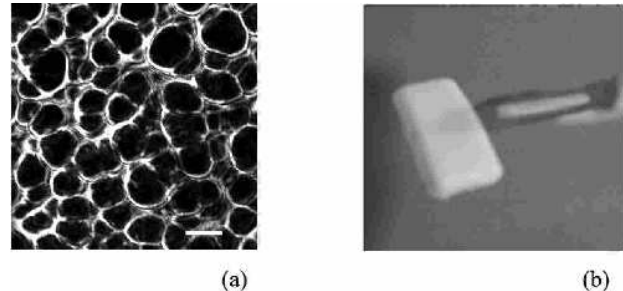


Fig. 1. (a) Reflection-mode confocal image of cellular structure in the 5CB nematic colloid at $\Phi = 10\%$ [1]. The white bar shows the length scale of $20\mu\text{m}$. (b) The photo of an aggregated 10%-5CB colloid, showing its white scattering appearance and the evident rigidity.

In any case, regardless of which structure the aggregating liquid crystal colloid adopts, the phase equilibrium and kinetics are altered in non-trivial ways due to the underlying frustrated liquid crystalline order. The cellular structure we find in our systems is, clearly, a metastable state. One of the main questions we address here is the change in rheological behaviour due to locally highly concentrated forces in the aggregated networks, creating high barriers to deformation. One may expect a glass-like freezing of motion and the resulting prolonged stability of the phases.

In contrast to the network supported by topological defects (disclinations), as in the recent study [5] of bigger aggregates and somewhat weak static modulus $G' \sim 0.01$ Pa, the cellular solids in our work possess a storage modulus of $G' \geq 10^5$ Pa. This solidification was first reported in [8] for a 5CB-PMMA colloid with particles of $R \approx 250$ nm. In this paper we present further results on the mechanical properties of nematic colloid, with smaller particles and fast quenching rates, showing the storage modulus approaching an even higher values, 10^6 Pa, and examining the yield and ageing properties of this phenomenon.

2 Experimental

The preparation procedures were described in some detail in the companion paper [1]. A typical thermotropic nematic liquid crystal 5CB (from Aldrich) has been mixed with monodisperse PMMA particles of radius $R = 150$ nm, sterically stabilised by chemically grafted poly-12-hydroxy stearic acid chains. Such short radially grafted polymers provide a homeotropic director anchoring. In all experiments we use the relatively small particle volume fraction, not more than $\Phi = 15\%$, determined by weight. Good mixing of particles was achieved above the nematic-isotropic transition and the samples were stored at $T \sim 45\text{C}$ (above $T_{\text{ni}} = 35.8\text{C}$ in pure 5CB) in a tumbling device to ensure that mixtures are homogeneous before any experiment is started.

An alternative colloid system has been prepared with another famous thermotropic nematic MBBA (Aldrich). We use this system for comparison, as an example of a ‘‘poor’’ nematic order in the supporting matrix (the MBBA is partially hydrolysed in ambient conditions, with effective $T_{\text{ni}} = 37.3\text{C}$ in pure MBBA), see [1] for detail.

The mechanical properties have been studied on a Dynamic Stress Rheometer, from Rheometrics Ltd, in the parallel plate set-up. A sinusoidal stress of low frequency is applied to the sample and the resulting strain is measured and interpreted by the software. Unfortunately, this device did not have an option to impose an oscillating strain of small constant amplitude. This prevented us from studying in detail the sample rheology during the nematic-isotropic transition and structure formation – the change in the modulus is so great (between ~ 0.01 and 10^5 Pa) that the constant-stress mode of the rheometer could not cope and the settings had to be adjusted below T_{ni} .

The rheometer was equipped with the purpose-made environmental stage allowing the rapid cooling of the sam-

ple (at a rate $35^\circ/\text{min}$). The experimental procedure was as following:

1) The sample was heated to $\sim 50\text{C}$ in an ultrasonic bath (to ensure homogeneous particle mixing) and then transferred, via a pre-heated syringe, to the pre-heated rheometer plate. The upper plate was then lowered slowly, to the gap ~ 0.5 mm. All through this manipulation, the temperature of the sample was remaining above its T_{ni} .

2) The environmental chamber was then closed and the temperature stabilised at 50C to return the sample to its isotropic mixed state. The oscillating movement of plates was started at this moment, with a low constant value of stress ~ 0.3 Pa since the isotropic suspension is a liquid with low viscosity, and a constant frequency of 1 Hz. Samples were allowed to equilibrate in this regime for at least 10 min.

3) The rheometer run was then stopped and the temperature quickly dropped to the working level, every time 15 degrees below T_{ni} (e.g. to 20C for $\Phi = 5\%$ and 18C for $\Phi = 15\%$ in 5CB). The rheometer was restarted at exactly 100 s after the working temperature was reached. A higher value of oscillating stress amplitude, $\sim 3 - 30$ Pa, was required to acquire reliable data on the resulting rigid cellular solid.

4) To study the yield stress behaviour, the same procedure of sample loading and quenching was followed. The rheometer was then set to perform a low frequency stress-sweep test, measuring the response of the system on increasing shear stress – thus reaching the point of breaking and yield of the cellular structure.

3 Results and discussion

The first observation that one makes on cooling the homogeneously mixed colloid suspension below the nematic-isotropic transition is the rapid optical change. Above T_{ni} the suspension with a low particle concentration is relatively transparent. Below the clearing point the colloid becomes completely opaque, white in the case of 5CB and marginally yellow for MBBA. Clearly, a strong multiple scattering of light takes place in the material – significantly greater than in a pure nematic liquid crystal, which is turbid due to the director thermal fluctuations [6]. Such an opaqueness is usually a signature of randomly quenched disorder in the nematic director field and is found, for instance, in nematic silica-gels [9] and polydomain nematic elastomers [10]. Our study of structure of the aggregated nematic colloid below T_{ni} in the companion paper [1] confirms this view: the director is anchored on the walls of the cellular structure, see fig. 1(a).

Secondly, we find the remarkable rigidity of the resulting material. Even before the detailed rheological study, one notices that the opaque aggregated colloid is solid. It evidently supports its own weight, fig. 1(b), one can cut it with a knife, imprint shapes and handle it quite robustly. An important unresolved question is of the ageing of such a system. In general, the prepared shape of the aggregated cellular solid is preserved for a long time, if

the temperature is kept constantly deep below T_{ni} . However, we observe that some amount of liquid (apparently, the pure liquid crystal) leaks from the samples over a period of days and weeks, the effect being much stronger in MBBA colloids than in 5CB ones, and at smaller particle concentrations.² In spite of this, the integrity of the sample solid shape seemed to be preserved. In this paper we do not discuss effects of ageing and leave it for another, more detailed research work.

A third general observation, made both during the uncontrolled cooling of the colloid mixture on the lab bench and in the environmental chamber of the rheometer, is that the rate of cooling has a strong effect on the resulting rigidity. Fast quenching, at least in the initial period after reaching the working temperature, makes the material much more rigid and the cellular structure more regular. The latter fact is obtained by comparing the confocal microscope images of cellular morphology of the same samples cooled on the bench and those taken from the rheometer after a fast quenching and parallel-plate rheometer run.

Finally, turning to the detailed study of the mechanical properties of aggregated cellular solids, we find that another crucial effect is the actual value of the working temperature: the storage modulus G' depends on it very strongly. This introduces a slight ambiguity in comparison of the data between colloids of different particle concentration, since they have their T_{ni} different, decreasing with the average volume fraction of a colloid mixture Φ [1]. We chose to work at a fixed difference below T_{ni} , but it is not clear that the resulting difference in absolute values of working T does not introduce a shift in G' . Due to this problem, one cannot be certain that the plots of G' against colloid concentration, figs. 2(b) and 3(b), are completely consistent and one should interpret them with a degree of caution.

3.1 Storage modulus

After following the same thermal history for all the samples, that is a rapid quench to 15° below their respective T_{ni} and a 100 s delay after this temperature was first reached, the complex modulus $G(\omega)$ of the aggregated cellular solids has been measured as a function of time. We are particularly interested in the storage modulus which, at low frequency such as $\omega = 1$ Hz, is a representative feature of the equilibrium elastic response. Of course, above T_{ni} , for a homogeneously mixed low-concentration colloid suspension, this storage modulus is essentially zero.

The resulting values of storage modulus G' are remarkably high for all materials and compositions studied – this solidification of a nematic colloid is the main result of this paper, illustrated in figs. 2 and 3. The accurate measurement of this modulus meets some unavoidable experimental difficulties: for a large G' , the stress applied to the

² In fact, there is quite a difference between the 5CB and MBBA colloids. The MBBA-material is much less robust, breaks, leaks liquid and does not have such a long “shelf-life” as the 5CB one.

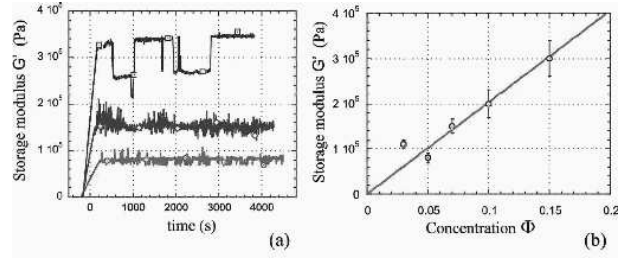


Fig. 2. The evolution with time of the storage modulus G' at constant frequency $\omega = 1$ Hz for the 5CB colloid at $\Delta T \approx 15^\circ$ below T_{ni} , for particle concentrations $\Phi = 5\%$, 7% and 15% , graph (a), curves with increasing saturation. Graph (b) shows the dependence of the saturation value G' on the particle concentration. A linear fit gives, $G' \sim (2 \times 10^6) \Phi$ Pa.

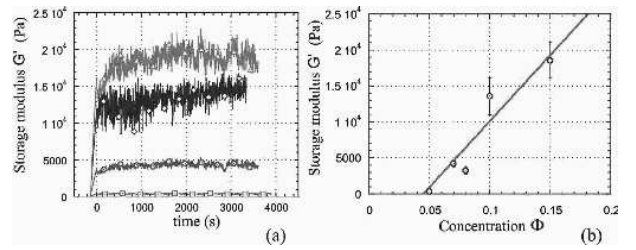


Fig. 3. The evolution with time of the storage modulus G' at constant frequency $\omega = 1$ Hz for the MBBA colloid at $\Delta T \approx 15^\circ$ below T_{ni} , for particle concentrations $\Phi = 5\%$, 7% , 10% and 15% , graph (a), curves with increasing saturation. Graph (b) shows the dependence of the saturation value G' on the particle concentration. An attempted linear fit gives $G' \sim (1.8 \times 10^5) [\Phi - 0.045]$ Pa.

rheometer plates has to be sufficiently high to produce a measurable strain. However, too high a stress results in the slipping of the plates, which become lubricated by the leaking nematic liquid, or the complete breaking of the cellular structure (the yield effect, discussed below). The compromise between these two trends leads to rather high experimental noise, especially in systems with higher particle concentration where the shear strain tends to be lower for an allowed range of applied stress.

The results for G' in 5CB and MBBA aggregated colloids show small variation of the modulus with time, at least during the first several minutes or hours. There is also a marked difference in values between the 5CB colloid and the “poor” nematic material based on partially hydrolysed MBBA. The elastic modulus is more than an order of magnitude lower in the MBBA colloid.

Formation of a rigid cellular solid proven, the final level of G' is related to the initial particle concentration. Figures 2(b) and 3(b) give such a dependence. The data points are somewhat scattered and are affected by a high noise, or experimental uncertainty. However, the linear dependence on concentration is a plausible conclusion for both 5CB and MBBA colloid aggregates. A striking difference between the two systems, apart from the magnitude of G' , is the apparent low-concentration threshold at

$\Phi \sim 4.5\%$ for the cellular aggregation of the MBBA colloid. This observation in the “poor” nematic model system is consistent with the phase diagram in fig. 9 of the companion paper [1]. There, examining the case of smaller strength of nematic field, one finds a noticeable region of miscibility at low concentrations, below T_{ni} . In contrast, for the Landau parameters characteristic of a “strongly nematic” 5CB, this region is too narrow to be practically observable – accordingly, the $G'(\Phi)$ dependence for 5CB suggests that it aggregates from nearly zero Φ .

At this point one may remark that the rheometric data obtained at a slow cooling rate [8] have shown a much lower values of storage modulus G' . Although there is a difference in colloid particle sizes (the authors of [8] used $R \approx 250$ nm, which should affect the aggregation kinetics and morphology), we also find that the rate of system quenching and the time the aggregating colloid spends at rest at the working temperature have a strong effect on the resulting strength of cellular structure.

3.2 Stability and Yield stress

The aggregated cellular structures of nematic colloids were very stable over the period of about an hour, as confirmed both by visual observation, constancy of confocal images and the little variation of measured G' with time. Over longer periods, one observes a “leaking” of pure liquid crystal from the rather rigid and completely opaque cellular aggregate. We did not study this effect in detail, but one may speculate that the open-cell morphology allows the nematic liquid to gradually find its way out of the over-constrained cellular environment.

However, from the moment of formation one observes a systematic step-like variation in the modulus, especially visible for 15% 5CB system in fig. 2(a). In this particular material the G' is so high that we had to apply a relatively high constant stress to obtain any measurable deformation response. One might argue that the the steps between two distinct values of 2.6 and 3.5×10^5 Pa are due to a partial breaking and reforming of the cellular structure.³

A different type of rheological experiment, a stress sweep at constant low frequency $\omega = 1$ Hz, allows to investigate the yield stress behaviour. In figs. 4(a) and 5(a) we plot the values of shear strain in response to the gradually increasing stress between the rheometer plates. The slope of the initial linear increase gives the value of G' . However, at higher stress the material yields. We identify the corresponding value of stress as the yield-stress σ_y , which is a function of colloid concentration. Once again, one finds a difference of more than an order of magnitude between the 5CB and MBBA materials.

Plotting the concentration dependence $\sigma_y(\Phi)$, figs. 4(b) and 5(b), we again find that the MBBA colloid shows a concentration threshold at $\Phi \sim 4.5\%$ [compare with

³ An alternative possibility of rheometer plate slipping was also frequently observed, but this always resulted in a rapid monotonic decline of measured G' to nearly zero – not the repeated steps as in fig. 2(a).

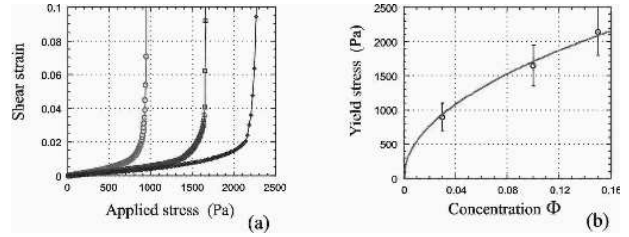


Fig. 4. The yield stress effect: (a) Strain-stress curves at a frequency $\omega = 1$ Hz for the 5CB colloid at $\Delta T \approx 15^\circ$ below T_{ni} , for particle concentrations $\Phi = 3\%$, 10% and 15% . (b) The yield stress vs particle concentration; solid line shows the fit $\sigma_y \approx (5400 \Phi^{1/2})$ Pa.

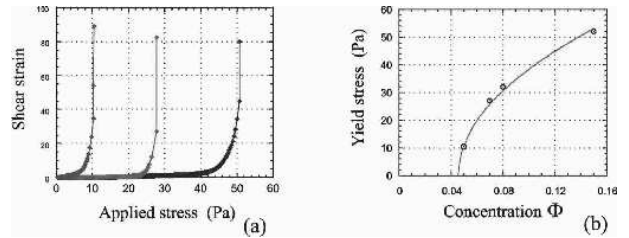


Fig. 5. The yield stress effect: (a) Strain-stress curves at a frequency $\omega = 1$ Hz for the MBBA colloid at $\Delta T \approx 15^\circ$ below T_{ni} , for particle concentrations $\Phi = 5\%$, 7% and 15% . (b) The yield stress vs particle concentration; solid line shows the fit $\sigma_y \approx (168 [\Phi - 0.045]^{1/2})$ Pa.

fig. 3(b)]. A good single-parameter fit to a square-root dependence $\sigma_y \propto \Phi^{1/2}$ is different from the scaling predicted by a crude theoretical model in Appendix. However, the magnitude of yield stress is in the correct range, appropriately much greater for 5CB colloids where the strong nematic field should generate a greater pressure on interfaces and thus preserve the particle dense packing.

4 Elastic response of cellular superstructure

First of all, one needs to appreciate the very large elastic modulus, which usually tells about a significant energy density stored in the aggregated nematic colloid. To illustrate the values, let us compare the characteristic energy scales involved. Assume, for the purpose of estimate, a 5% volume fraction of colloid particles with 150 nm radius. The director field around each particle contains the elastic energy $\sim 10 KR$ in the case of strong anchoring, or $\sim 0.2 W^2 R^3 / K$ in the case of weak anchoring, [11]. Therefore, even the energetically most unfavourable case of separate, equidistant particles (separation $d \sim 4R$ at 5%) results in the energy density $\sim 0.16 K / R^2 \sim 60$ Pa. In reality, particles would always aggregate in some way, significantly reducing this estimate (e.g. particles lumped in the nodes of disclination network in [5] are separated by $d \sim 100 \mu\text{m}$, giving the energy density of just ~ 0.01 Pa). Also, considering that the particles of this size will have the colloid parameter $WR/K \ll 1$, it is far more likely that the case of weak anchoring would occur and even the separate equidistantly distributed colloid would have the

elastic energy density of only $\sim 3 \times 10^{-3} W^2/K \sim 10^{-4}$ Pa. None of these values can even crudely account for the large values of elastic modulus G' observed in nematic colloids.

Of course, it is not the energy density itself, but the rate of its change – a slope of energy variation with deformation, that determines the modulus. We now try to outline the physical origin of such variation. It seems clear that the dramatic enhancement of mechanical properties is due to the cellular structure of phase-separated nematic colloids. Particles, densely packed and solidified on thin interfaces, produce very high surface tension γ . There are several processes contributing to this surface tension.

(1) Let us first consider the local melting of the nematic phase. The gaps between closely packed particles are of order or less than $\xi \sim 10$ nm, the characteristic nematic correlation length. The nematic liquid in these small gaps is melted, cf. fig. 6(a) and the phase diagram in ref. [1]. The thermodynamic energy density of a melted nematic at $T < T_{ni}$, ΔF_n is obtained from the mean-field energy part of eq. (7) of [1]; qualitatively

$$\Delta F_n \simeq \frac{(A_o T^*)^2}{4C} \frac{1 - \tau}{\tau} \sim 10^7 (1 - \tau) \text{ J/m}^3, \quad (1)$$

with $\tau = T/T^*$. The last estimate in (1) is based on the Landau parameters given in [1]. The $(1 - T/T^*)$ factor, of course, is only valid near the nematic transition, where the variation of order parameter $Q^*(T)$ is significant. The effective surface tension of such an interface is a result of increasing the relative volume occupied by the dense phase (assuming the constant interface thickness nR) with the melted nematic in the gaps between particles:

$$\gamma_n \approx (1 - \phi_c)(nR)\Delta F_n, \quad (2)$$

where $(1 - \phi_c)$ measures the amount of volume left for the nematic liquid in the cell wall (ϕ_c being the particle close-packing volume fraction).

(2) The imbalance in energy density between the pure nematic inside cells on both sides of isotropic interfaces and the isotropic melt inside these densely packed interfaces acts as an effective pressure of a magnitude $\sim \Delta F_n$. This effect would compress the interfaces, trying to reduce the volume occupied by the unfavourable melted state. This situation is analogous to the process of packing of granular matter by gravity or external pressure. Taking our monodisperse spherical particles, the results are that the maximal particle volume fraction is reached at random close packing $\phi_c \approx 0.64$, when there are on average the maximal possible number of contacts, $N_c \approx 8.6$, between the spheres. The contacts create a depletion gap in the free energy, see Appendix and fig. 6(b). The resulting cusped minimum is very narrow because the dependence of packing concentration on the number of contacts is very sharp [12, 13]. These, and other theories of granular matter provide a number of advanced estimates, some valid over a large range of concentrations well below ϕ_c . One may take a view that a crude linear estimate $N_c \approx N_{\max} + \beta(\phi - \phi_c)$ can be obtained simply by considering that $N_c \rightarrow 0$ already at $\phi \sim 0.5$. This gives the (lower bound) estimate for the slope: $\beta \sim 100$.

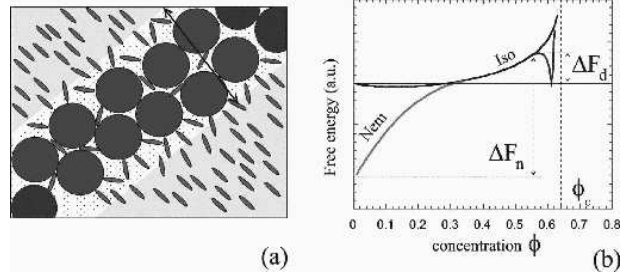


Fig. 6. (a) Model of cell border close-packed with colloid particles – the thin interface between clean nematic domains. The interface thickness is related to the particle size, $d = nR$, with $n \sim 4$ in the sketch. The remaining space in the interface is filled with the matrix liquid in its isotropic state. (b) The plot of free energy $F(\phi)$ (see [1] for detail) showing the difference in local nematic mean field energy density ΔF_n . The plot also shows the cusped minimum of depth ΔF_d resulting from the depletion locking between particles in contact (see text and Appendix)

The narrow cusped structure of the free energy at the high- ϕ end of phase diagram provides the additional reason for the effective surface tension of interfaces, γ_d , and also gives the expression for the yield stress σ_y . The interface tension is estimated by the following argument: Take the value for the energy of a single depletion gap eq. (6) and use the estimated linear dependence for the number of contacts $N_c(\phi)$. We can now describe the local free energy density increase in response to the change (decrease) in local particle volume fraction $(\phi - \phi_c)$

$$F \approx \frac{(\gamma_o R a)\phi_c}{v_R} N_c = F_{\min} + \frac{\beta(\gamma_o R a)\phi_c}{v_R} (\phi_c - \phi). \quad (3)$$

The particle concentration can be related to the local change in surface area $\delta\mathcal{A}$, namely $\phi - \phi_c \approx -\phi_c \delta\mathcal{A}/\mathcal{A}_c$, assuming its constant thickness and the “equilibrium” close-packing area \mathcal{A}_c ⁴. Then the change in the full free energy on stretching the interface can be written as

$$(F - F_{\min})V \approx \frac{\beta\gamma_o R a \phi_c^2}{v_R \mathcal{A}_c} V \delta\mathcal{A} \sim \frac{\beta\gamma_o a \phi_c^2 \lambda}{R^2} \delta\mathcal{A} \quad (4)$$

$$\gamma_d \approx \frac{\beta\gamma_o a \phi_c^2 \lambda}{R^2}$$

where v_R is the particle volume and $\lambda = V/\mathcal{A}_c$ the cell size. In this way, the eq. (4) identifies the effective surface tension γ_d resulting from a local energy increase due to the rapid loss of particle contacts on stretching the interface.

We have a cellular solid system with interfaces under tension (rather than, say, elastic walls as in [14]), with open cells, so that the conservation of cell volume is not posing a constraint. The elastic modulus of such a system

⁴ Take the current density of interface of constant thickness nR to be $\phi = N/V$. Then

$$\phi = \frac{N}{nR(\mathcal{A}_c + \delta\mathcal{A})} \approx \frac{N}{nR\mathcal{A}_c} \left(1 - \frac{\delta\mathcal{A}}{\mathcal{A}_c}\right) \equiv \phi_c(1 - \delta\mathcal{A}/\mathcal{A}_c).$$

is estimated as $G' \simeq \gamma/\lambda$, where $\gamma = \gamma_n + \gamma_d$ is the total effective surface tension of cell walls and the mesh size $\lambda \sim nR/\Phi$. We thus obtain from the two physically different contributions to the surface tension:

$$G' \approx (1 - \phi_c) \frac{(A_o T^*)^2 (1 - \tau)}{4C\tau} \Phi + \frac{\beta\gamma_o a \phi_c^2}{R^2} \quad (5)$$

$$\sim [10^6(1 - \tau)\Phi + 10^5] \text{ Pa} .$$

The numerical estimate is obtained for the material parameters of 5CB, cf. the Appendix of ref. [1]. The experimental data of figs. 2(b) and 3(b) suggest that deep below the nematic transition of a classical thermotropic nematic material, the dominant factor is the energy of nematic melting and, thus, the elastic modulus G' is a linear function of colloid concentration ϕ . On the other hand, close to T_{ni} , when $\tau \rightarrow 1$, the modulus should become a concentration-independent material constant determined by the packing of hard spheres under pressure.

One of the consequences of the depletion mechanism is the effect of the nematic order $Q(T)$, and of small vibrations. This mechanism is based on the particle packing approaching the random close packing limit ϕ_c and having a very sharp dependence of average number of depletion contacts on local concentration. It is known that the packing density increases sharply when the sandpile is subjected to an external pressure (the role often played by the gravity body force) and the vibrations. In our case, the nematic mean field creates such an effective pressure. We expect, and indeed find in the experimental study of cellular structure [1], that a small-amplitude oscillating strain in the rheometer makes the cells much more uniform and interfaces visibly sharper.

5 Conclusions

We have reported results of investigation of mechanical properties of new cellular solid aggregates of liquid crystal colloids quenched below their clearing point. Two main conclusions can be made from this study. The magnitude of the low-frequency storage modulus, which is comparable with that of a normal rubber, indicates that the thin cell walls possess an unusually high effective surface tension. Theoretical arguments suggest that the main mechanism for such a local increase in energy density is the local melting of nematic liquid, making G' a linear function of average colloid concentration. The second important result of this paper is the yield behaviour of cellular macrostructure and the dependence of the yield stress on concentration. Qualitative arguments suggest a possible mechanism for the observed yield stress. However, within the limited accuracy of our experiments, we observed a concentration dependence $\sigma_y \propto \Phi^{1/2}$ which is not accounted for by the crude depletion model.

An interesting comparison can be made between the colloids based on ‘‘good’’ and ‘‘poor’’ nematic matrix. Not only the values of elastic modulus and the yield stress are much lower in the MBBA system, but we also observe a characteristic threshold concentration $\Phi \sim 4.5\%$ below

which the MBBA colloid does not phase separate into the cellular structure.

We must emphasize a number of experimental difficulties in the study of mechanical properties of our cellular solids. The rheometric results, even for the same batch of colloid, are often not reproducible. The reasons are the important role of the rate of quenching and, specifically for the parallel-plate rheometric experiment, slipping of plates lubricated by the nematic liquid. It is possible that an alternative approach, for instance examining the mechanical response to an indentation probe rather than the sheared plate, will give a better defined experiment.

Notwithstanding these uncertainties, we have observed the unusual phase behaviour and remarkable rheological response in the ‘‘classical’’ liquid crystal colloid – a straightforward low-concentration mixture of thermotropic nematic with sterically stabilised PMMA particles. The metastable cellular solid aggregates are preserved by thermodynamic forces provided by the nematic mean field. No doubt, further investigations into the mechanisms of cellular structure formation and its stability would make possible a controlled, reliable and robust preparation of a wide variety of new materials.

We appreciate valuable discussions with M.E. Cates, S.M. Clarke and P.D. Olmsted. This research has been supported by EPSRC UK.

Appendix: Depletion gap in densely packed walls

Another effect that switches on when the particles come into close contact on localised interfaces is the depletion reduction of their surface energy. When isolated in the nematic solvent matrix, each particle’s surface has the energy of the order $\gamma_o(4\pi R^2)$, with γ_o the main surface tension of, e.g. hydrocarbon PHSE and biphenyl oil interface; qualitatively the value of this tension is of the order $\gamma_o \sim 0.05 \text{ J/m}^2$ [15] and far exceeds all anisotropic anchoring corrections. In the Deryagin approximation, each contact between two particles creates a depletion disk and reduces this energy by $\sim 2\gamma_o R a$, where $a \sim 1 \text{ nm}$ is the size of the molecule of suspending liquid. In the randomly close-packed state each particle has $N_c \sim 8.6$ contacts (the never-reached absolute maximum would be $N_c = 12$ for fcc packing) which, for a cell wall of thickness nR , gives the depletion gain in the local potential energy density

$$\Delta F_d \sim N_c(\gamma_o R a) \frac{\phi_c}{R^3} \sim 5 \times 10^3 \text{ J/m}^3 \quad (6)$$

This gap would continuously deepen on increasing the number of contacts. However, the maximal number N_c is reached at close packing and cuts this linear decrease, thus creating a cusped minimum of the free energy density, shown in fig. 6(b). The depth of the minimum (6) gives an estimate for the yield stress: when the interface is distorted such that the particles lose most of their contacts, the high resistance to deformation is lost and the cellular

structure would no longer be stable. Taken in proportion to the total amount of interface in the cellular structure, the macroscopic yield stress should be a function of initial concentration of the colloid:

$$\sigma_y \sim \Phi \Delta F_d \sim 200 \text{ Pa.}$$

One should appreciate that the estimates here are extremely crude, and yet they give not an unreasonable value $\sigma_y \ll G'$.

References

1. V.J. Anderson, E.M. Terentjev, S.P. Meeker, J. Crain and W.C.K. Poon, the companion paper on “morphology”.
2. P.E. Cladis, M. Kleman and P. Pieranski, *C. R. Acad. Sci. Paris* **273** (1971) 275.
3. P. Poulin, V.A. Raghunathan, P. Richetti and D. Roux, *J. Physique II* **4** (1994) 1557.
4. P. Poulin and D.A. Weitz, *Phys. Rev. E* **57** (1998) 626.
5. M. Zapotocky, L. Ramos, P. Poulin, T.C. Lubensky and D. Weitz, *Science* **283** (1999) 209.
6. P.G. de Gennes and J. Prost, *Physics of Liquid Crystals* (Clarendon, Oxford, 1993).
7. H. Tanaka and J. Yamamoto – to be published (2000)
8. S.P. Meeker, W.C.K. Poon, J. Crain and E. Terentjev, *Phys. Rev. E* (2000) accepted.
9. T. Bellini, N.A. Clark, C.D. Muzny, et al., *Phys. Rev. Lett.* **69** (1992) 788.
10. E.M. Terentjev, *J. Phys. C: Cond. Matter* **11** (1999) R239.
11. O.V. Kuksenok, R.W. Ruhwandl, S.V. Shiyonovskii and E.M. Terentjev, *Phys. Rev. E* **54** (1996) 5198.
12. S. Torquato, *Phys. Rev. Lett.* **74** (1995) 2156.
13. J.X. Liu and T.J. Davies, *Powder Metallurgy* **40** (1997) 48.
14. M.F. Ashby and L.J. Gibson, *The mechanical properties of cellular solids* (Cambridge University Press, 1983).
15. *Treatise on Solid State Chemistry*, ed. N.B. Hannay, Vol. 6B - Surfaces II (Plenum Press, N.Y. - London, 1976).